

Modified approach to the construction of a blue noise mask

Meng Yao

Kevin J. Parker

University of Rochester

Center for Electronic Imaging Systems

Department of Electrical Engineering

Rochester, New York 14627

Abstract. *The blue noise mask (BNM) is a halftone screen that produces unstructured, visually pleasing halftone images. Since it is a point process, halftoning using the BNM can be implemented considerably faster than error diffusion and other algorithms. However, in the construction of the original BNM, a number of constraints were used to limit its characteristics in the spatial and frequency domains. These constraints were not efficient to compute and required adaptability to all gray levels in the construction process. The original BNM also contained some small but unwanted low-frequency components at some gray levels. In this paper, we present a revised approach to the generation of blue noise patterns and the construction of BNMs employing more efficient computations and eliminating more unwanted residual low-frequency components. Psychovisual evaluation shows that dithering with the new BNM gives excellent results and its rating is statistically indistinguishable from that of error diffusion with serpentine raster and perturbed weights.*

1 Introduction

It is accepted in halftoning that unstructured, high-frequency (blue noise) dot patterns are visually pleasing. Error diffusion,¹ a halftone algorithm that produces high-quality halftone images, has been shown to have blue noise characteristics in the transform domain.^{2,3} More sophisticated algorithms that make use of error diffusion have been proposed to improve its quality, such as those introduced by Ulichney,² Eschbach and Knox,⁴ and Pappas and Neuhoff.⁵ Generally, these add to the computation complexity of error diffusion. Sullivan, Ray, and Miller⁶ used a visual criterion

to generate blue noise patterns, but the halftone process involves a gamut of halftone patterns for all gray levels instead of a single halftone screen. Rolleston and Cohen⁷ generated a halftone screen with correlated (high-frequency) noise; however, the halftone patterns at individual levels were not constrained to blue noise patterns. The blue noise mask (BNM) reported by Mitsa and Parker is distinct in that the halftone pattern of the BNM at each level has constrained first-order (the gray level is preserved) and second-order (the power spectra have blue noise characteristics) statistics^{8,9} and, therefore, blue noise is explicitly guaranteed in its binary pattern at each level. The halftone process of the BNM is a simple comparison of the image pixel value against the corresponding mask value, just like other ordered-dither methods, but it is free of periodic structures that normally exist in ordered dither¹⁰ and its blue noise characteristic produces unstructured dot patterns comparable to those of error diffusion.⁹ However, a number of improvements are possible that make construction of new BNMs more efficient, reduce further any residual low-frequency artifacts, and add desirable features of the human visual system (HVS).

Briefly, the original BNM was constructed for one gray level at a time beginning with an intermediate starting binary pattern, or *seed*. Each subsequent level was constrained by the binary pattern at a preceding level, such that a single-valued function, or ordered-dither array, was constructed with desired first-order and second-order statistics. At each level, a circularly symmetric filter was used to identify and eliminate low-frequency structures (large “clumps”) incompatible with the desired blue noise power spectrum. Implicit periodicity, or “wraparound” filtering, was used so the BNM could be seamlessly tiled with itself to cover larger image spaces.^{8,9} These concepts were later adapted and employed

Paper 93-047 received July 8, 1993; revised manuscript received Nov. 9, 1993; accepted for publication Dec. 1, 1993.
1017-9909/94/\$6.00. © 1994 SPIE and IS&T.

by Ulichney,¹¹ who used the term *voids and clusters* to describe the unwanted low-frequency structures (“clumps”) in a BNM construction.

In the original report by Mitsa and Parker,^{8,9} spatial constraints such as local means were also employed as redundant enforcement of desired properties of the binary pattern. These filters were adaptive with respect to gray level and also with respect to the individual binary patterns found at the start of each level of construction. This paper describes a simpler approach where a simple anisotropic filter is used without any adjunct constraints. Also, the filter is adaptive over gray levels, but not with respect to the details of each binary pattern formed in the construction steps. These modifications eliminate some capability to shape details of the desired power spectrum of a binary pattern, but make the overall processing more simple, enabling turnkey construction of independent BNMs. Another modification is the inclusion of the anisotropy of the HVS with respect to angle. In the binary pattern power spectrum, more energy can be placed at the diagonal since the HVS has its weakest high-frequency response there. The results will be shown to be quantitatively and qualitatively improved with respect to results from error diffusion rendering and the original BNM.

2 New BIPPSMA

In this section, we present a new BIPPSMA (*Binary Pattern Power Spectrum Manipulating Algorithm*), which can convert any binary pattern at any level to a blue noise pattern. The new BIPPSMA differs from the one by Mitsa and Parker⁹ in that the latter tries to force the binary pattern into the pre-defined isotropic blue noise power spectrum, with negligible low-frequency energy, and a prescribed high-frequency level of the radially averaged power spectrum. The new BIPPSMA uses a simple anisotropic filter to eliminate low-frequency energy, without prescribing the details of the high-frequency level. In this way, the clumps in the binary pattern are removed and the resulting pattern will be a visually pleasing blue noise pattern. Specifically, starting with an initial binary pattern, such as white noise, we take the fast Fourier transform (FFT) of the current pattern, filter it in the frequency domain, and take the IFFT back to the spatial domain where the values will now be different from those of the binary pattern and are no longer binary. For all pixels with a 1 (corresponding to white dots) in the binary pattern, we find the pixels of the filtered array that have the largest positive deviation from the average gray level of the binary pattern. These are the centers of the largest white clumps. Similarly, for the 0’s (corresponding to black dots) in the binary pattern, we find the pixels with the largest negative deviation from the gray level of the binary pattern. These are the centers of the largest black clumps. We convert the values of clump centers and thus diminish the clumps. This process is repeated until a stopping criterion is satisfied, and our final binary pattern will have the qualities of the desired good pattern.

The steps of BIPPSMA are outlined as follows:

1. Set the initial number M of pairs of 1’s and 0’s to be swapped in each iteration.
2. Specify in the transform domain a 1-D low-pass filter appropriate for the gray level.
3. Rotate the 1-D filter to make the 2-D low-pass filter.

4. Take the FFT of the current binary pattern.
5. Filter the binary pattern with the 2-D low-pass filter.
6. Take the IFFT of the filtered pattern.
7. Form an error array by computing the difference between the filtered pattern and the gray level the pattern represents.
8. Sort the errors into two cases:
 - For all pixels containing a 1 in the binary pattern, sort the positive errors.
 - For all pixels containing a 0 in the binary pattern, sort the negative errors.
9. Swap the M pairs of 1’s and 0’s that have the highest positive and negative errors.
10. Compute the mean squared error (MSE) of the filtered pattern with respect to the gray level:
 - If the MSE drops, go to step 4 and proceed to the next iteration.
 - If the MSE increases and $M \neq 1$, reduce M by half, go to step 4.
 - Otherwise, stop.

The low-pass filter we use is any smoothly varying low-pass filter, such as a Butterworth, a Gaussian, etc., in which the cutoff frequency is adapted to the gray level of the binary pattern. According to Ulichney,³ a blue noise pattern has a principal frequency dependent on gray level:

$$f_g = \begin{cases} \sqrt{g}/R & \text{for } g \leq 1/2 \\ \sqrt{1-g}/R & \text{for } g > 1/2 \end{cases}, \quad (1)$$

where g is the gray level normalized to 1, and R is the distance of the addressable points on the display.

The principal frequency is considered to be a cutoff frequency for a blue noise power spectrum. We use it as a parameter in our low-pass filter. For the Butterworth filter:

$$F(u,v) = \left\{ \frac{1}{1 + \left[\frac{(u^2 + v^2)^{1/2}}{f_c} \right]^{2N}} \right\}^{1/2}, \quad (2)$$

where u and v are the transform coordinates, f_c is the cutoff frequency and N is the order of the Butterworth filter. Figure 1 shows the binary pattern at level 245 (95.7% of 256) with $f_c = 0.4 \times f_g$ and $N = 3$ for the Butterworth filter. For the Gaussian filter:

$$F(u,v) = \exp\left(-\frac{u^2 + v^2}{2\sigma^2}\right), \quad (3)$$

where σ is a function of the principal frequency. Figures 2 and 3 show the binary patterns at level 245 with $\sigma = f_g/4.5$ and $\sigma = f_g/2.5$, respectively. We see both filters yield very good results when the parameters are appropriately chosen.

The characteristic of the HVS can also be incorporated into the filter. We know that the human eye has maximum sensitivity in the horizontal and vertical directions and minimum sensitivity in the diagonal direction.¹² Thus we can

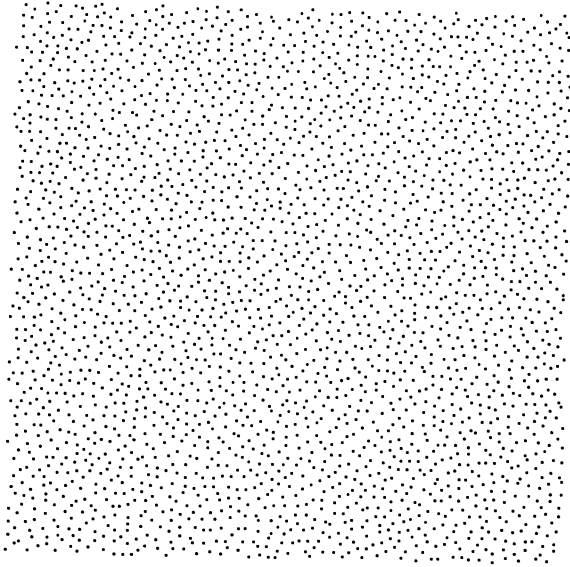


Fig. 1 Binary pattern at level 245 obtained with the Butterworth filter ($f_c = 0.4 \times f_g$ and $N = 3$).

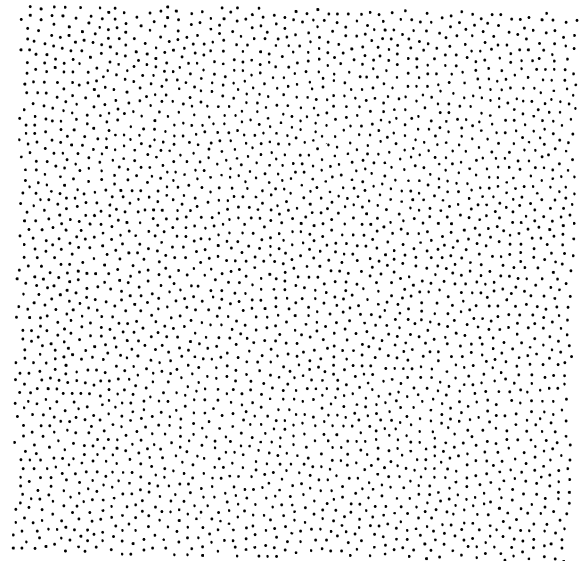


Fig. 3 Binary pattern at level 245 obtained with the Gaussian filter ($\sigma = f_g/2.5$).

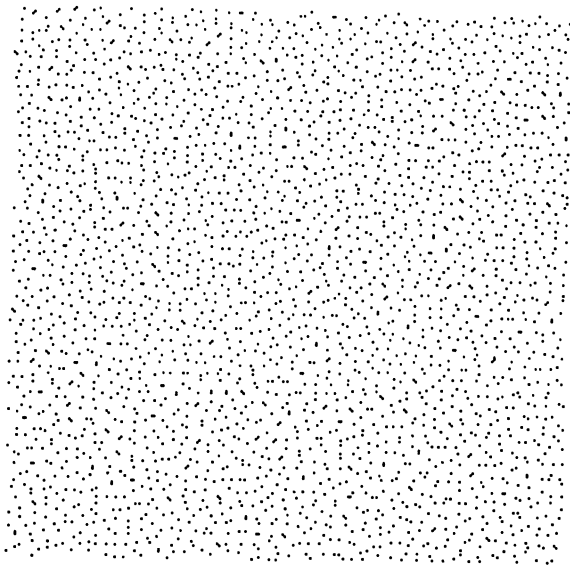


Fig. 2 Binary pattern at level 245 obtained with the Gaussian filter ($\sigma = f_g/4.5$).

add another parameter in our filter so that the filtered pattern will have more energy in the diagonal direction than in the horizontal and vertical directions:

$$F'(u, v) = [1 + c \times \cos(4\theta)] F(u, v) \quad (4)$$

where θ is the central angle around the dc point and c is a constant between 0 and 1 that controls the amount of energy redistribution. We found empirically that $c = 0.2$ is a good value to use. When $c = 0$, this reduces to our previous radially symmetric filter. The filter has smaller values in the diagonal direction and larger values in the horizontal and vertical directions, so the filtered binary pattern will have more energy in the diagonal direction and less energy in the horizontal and vertical directions due to the swapping step described.

Figure 4 shows the patterns obtained with $c = 0.3$ using the Gaussian filter with $\sigma = f_g/2.5$. Figures 1 through 4 all use a white noise pattern as the starting pattern.

The number of 1's and 0's swapped in each iteration will be reduced at certain points in the iteration process. We start with a relatively large number (e.g., 512 out of a 256×256 array) and when the MSE no longer decreases, this number is reduced by half and the MSE starts to decrease again. We continue this process until this number is 1 and the MSE stops decreasing. This will speed up the program and remove the clumps more cleanly than if a fixed number is used.

3 BNM Construction

To make the BNM, we need a good initial pattern $bp[i, j, g_s]$ for an intermediate level g_s ($0 < g_s < 255$, assuming 8-bit image planes), which we can obtain using BIPPSMA. From this initial pattern, we create an initial mask $m[i, j]$, which when used to halftone the constant gray level image of level g_s should produce the initial binary pattern. Then we move from level g_s to its higher levels. We create the blue noise pattern for the current level based on the binary pattern for the previous level by converting the appropriate number of 0's to 1's in the previous pattern. At the same time, the mask is updated. We continue this process until the mask has been updated for all the levels above g_s to level 255. Analogous procedures are used to construct the mask for all the levels below g_s . The resulting single-valued function will be our final BNM.

The initial mask is given by:

$$m[i, j] = \begin{cases} g_s, & \text{for } bp[i, j, g_s] = 0 \\ g_s - 1, & \text{for } bp[i, j, g_s] = 1 \end{cases} \quad (5)$$

where $bp[i, j, g_s]$ is the value of the binary pattern at level g_s at location $[i, j]$ and $m[i, j]$ is the mask value at location $[i, j]$.

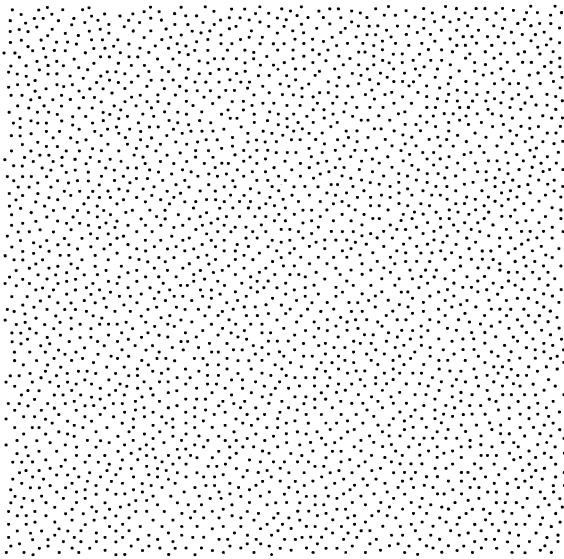


Fig. 4 Binary pattern at level 245 obtained with the Gaussian filter ($\sigma = f_g/2.5$ and $c=0.3$).

The steps for making the new BNM for $g > g_s$ are outlined as follows:

1. Set the number M of pairs of 1's and 0's to be swapped in each iteration.
2. Specify the 1-D low-pass filter appropriate for level $g_l + \Delta g$.
3. Rotate the 1-D filter with anisotropy to make the 2-D filter.
4. Create the initial binary pattern for level $g_l + \Delta g$ by converting randomly K 0's to 1's in the binary pattern for g_l (where $K = W \times W/L$, $W \times W$ is the size of the BNM and L is the total number of levels).
5. Take the FFT of the binary pattern for level $g_l + \Delta g$.
6. Filter the current binary pattern with the 2-D filter appropriate for level $g_l + \Delta g$.
7. Take the IFFT of the filtered pattern.
8. Form an error array by computing the difference between the filtered pattern and $g_l + \Delta g$.
9. Sort the errors into two cases:
 For the K 1's that are in the binary pattern for level $g_l + \Delta g$ but not in the binary pattern for g_l , sort the positive errors.
 For the 0's in the binary pattern, sort the negative errors.
10. Swap the M pairs of 1's and 0's that have the highest positive errors and negative errors.
11. Compute the MSE of the filtered pattern with respect to the gray level $g_l + \Delta g$.
 If the MSE drops, go to step 5 and proceed to the next iteration.
 If the MSE increases but $M \neq 1$, reduce M by half, go to step 5.
 Otherwise, go to step 12.

12. Update the mask:

$$m[i, j] = m[i, j] + \overline{bp[i, j, g_l + \Delta g]} ,$$

where the bar is the NOT operation.

13. If $g_l + \Delta g < 255$, let $g_l = g_l + \Delta g$, reset M , and go to step 2.

For constructing a mask for levels where $g < g_s$, the status of the 1's and 0's is opposite that of the upward case and the updating of the mask is given by:

$$m[i, j] = m[i, j] - bp[i, j, g_l - \Delta g] .$$

Other than that, the downward construction is basically the same as the upward construction.

Although we move from level g_l to $g_l + \Delta g$ by picking randomly K 0's and changing them to 1's, the iteration process using BIPPSMA will switch locations to eliminate clumps.

There is a significant constraint on BIPPSMA in the construction of the BNM. In making the BNM, the binary patterns at different levels are correlated. For example, in the upward construction, all the 1's in the binary pattern for level g_l are contained in the binary pattern for level $g_l + \Delta g$, so when we swap the 1's and 0's, these common 1's shared by the two neighboring levels cannot be changed. This is a requirement for the creation of the mask as a single-valued function.

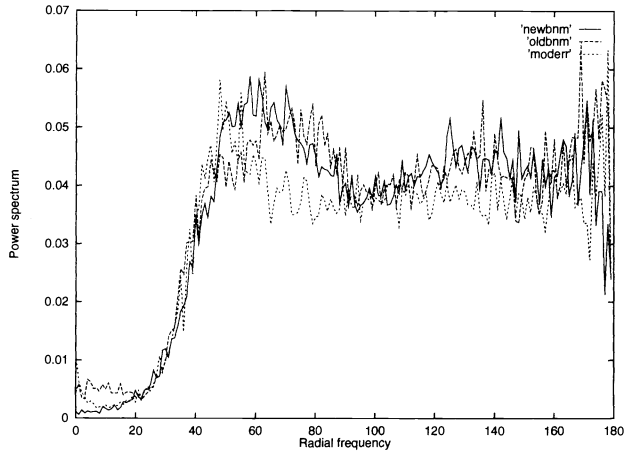
These construction techniques are quite general and have enabled the generation of BNMs with different properties such as 8-bit depth (0 to 255), 12-bit depth (0 to 4095), smaller size (64×64), larger size (256×256), isotropic ($c = 0$), and anisotropic ($c = 0.2$), and these can be selected to suit specific printer hardware configurations.

The construction techniques described are simple to implement and result in less residual low-frequency noise and more visually appealing properties than the earlier procedures for generating the original BNM.

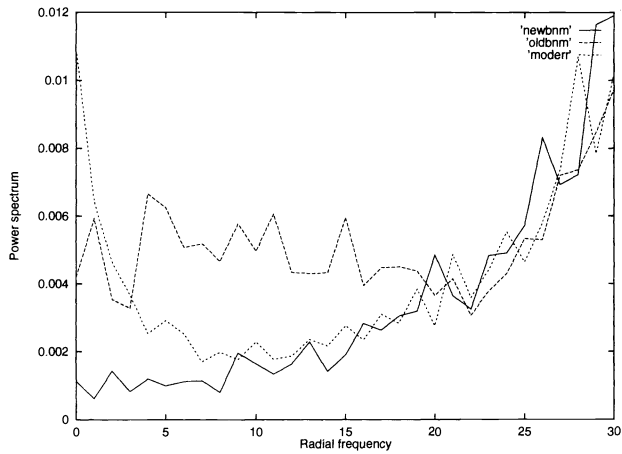
Figure 5(a) shows the radially averaged power spectra of a new BNM, the original BNM, and the modified error diffusion at level 245. A blowup of the low-frequency region is shown in Fig. 5(b). Note that the new BNM has the least energy in the low-frequency regions.

4 Psychovisual Evaluation

The new BIPPSMA and BNM construction are based on a single filtering operation that mimics the visual evaluation of uniformity and the anisotropy of the HVS. Because of this, we postulate that the results of the new BNM rendering should approach those of error diffusion, which is regarded to be a high-quality rendering technique under certain circumstances.¹³ To evaluate this, we presented six images to 11 viewers as (1) 8-bit gray-scale images, (2) 1-bit black-and-white images halftoned using the new BNM, and (3) 1-bit black-and-white images halftoned using error diffusion with serpentine raster and perturbed weights. The 8-bit gray-scale images were printed using a Kodak XL7700 contone printer, and the halftoned images were printed at 300 dpi using a Calcomp ColorMasterPlus. The images were typically $1k \times 1k$ pixels in size and were high-quality scanned photographs. The halftoned images were presented to the viewer

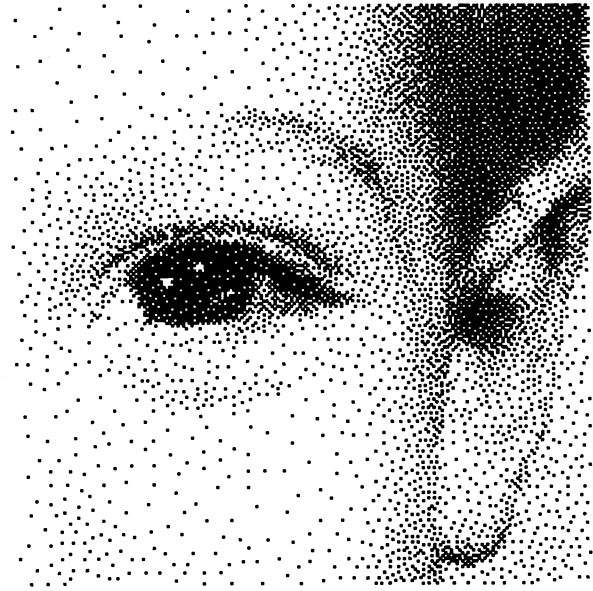


(a)

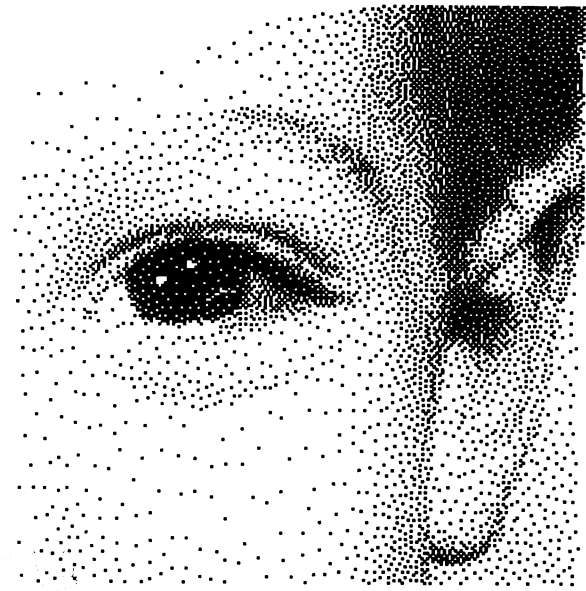


(b)

Fig. 5 (a) The radially averaged power spectra of a new BNM, the original BNM, and the modified error diffusion at level 245. (b) Blowup of low-frequency region in part (a).



(a)



(b)

Fig. 7 Zoomed section of a test image halftoned using (a) the new BNM and (b) modified error diffusion.

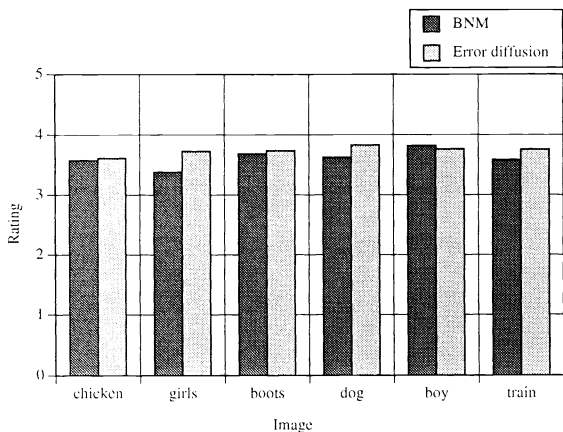


Fig. 6 The ratings of a new BNM and modified error diffusion for six images.

in a random order under identical conditions and the viewer rated the halftoned images based on their similarity to the original gray-scale images. A rating scheme from 5 to 1 was used, where 5 corresponded to an excellent rendition, 4 to good, 3 to fair, 2 to poor, and 1 to a bad rendition.¹⁴ The viewers were told that the contone image represented a score of 5. Figure 6 shows the average scores of the new BNM and error diffusion for each image. Figures 7(a) and 7(b) show a zoomed section of one of the test images using the new BNM and modified error diffusion, respectively. To see how close in quality the new BNM and error diffusion are, we have performed a two-tailed paired T-test¹⁵ on our data. Using

the 5% level of significance, we found that the T-test results do not indicate that one of the halftone methods is significantly different from the other in quality.

5 Conclusion

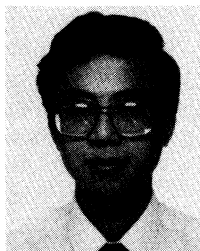
A modified approach to the generation of blue noise binary patterns and the construction of a BNM has been presented. It is simple since the filtering uses one criterion, which is preset and adaptive with respect to the gray level. It is also computationally efficient. It better matches the human visual response and hence produces improved patterns. Psycho-visual evaluation shows excellent ratings for the new BNM compared with the modified error diffusion approach.

Acknowledgments

This work was supported in part by the Department of Electrical Engineering, University of Rochester, and by NSF/NYS/Industry Center for Electronic Imaging Systems.

References

1. R. W. Floyd and L. Steinberg, "An adaptive algorithm for spatial gray-scale," *Proc. Soc. Inf. Displ.* **17**, 75-77 (1976).
2. R. A. Ulichney, "Dithering with blue noise," *Proc. IEEE* **76**, 56-79 (1988).
3. R. A. Ulichney, *Digital Halftoning*, MIT Press, Cambridge, MA (1987).
4. R. Eschbach and K. T. Knox, "Error-diffusion algorithm with edge enhancement," *J. Opt. Soc. Am. A* **8**, 1844-1850 (1991).
5. T. N. Pappas and D. L. Neuhoff, "Least-squares model-based halftoning," *Proc. SPIE* **1666**, 165-176 (1992).
6. J. Sullivan, L. Ray, and R. Miller, "Design of minimum visual modulation halftone patterns," *IEEE Trans. Syst. Man Cybern.* **SMC-21**(1) 33-38 (1991).
7. R. J. Rolleston and S. J. Cohen, "Halftoning with random correlated noise," *J. Electron. Imag.* **1**(2), 209-217 (1992).
8. T. Mitsa and K. J. Parker, "Digital halftoning using a blue-noise mask," *Proc. SPIE* **1452**, 47-56 (1991).
9. T. Mitsa and K. J. Parker, "Digital halftoning technique using a blue-noise mask," *J. Opt. Soc. Am. A* **9**, 1920-1929 (1992).
10. B. E. Bayer, "An optimum method for two-level rendition of continuous-tone pictures," *Proc. IEEE Int. Conf. Commun.*, pp. 26-11-26-15 (1973).
11. R. A. Ulichney, "The void-and-cluster method for dither array generation," *Proc. SPIE* **1913**, 332-343 (1993).
12. F. Campbell and J. Kulikowski, "Orientation selectivity of the human visual system," *J. Physiol.* **187**, 437-445 (1966).
13. J. F. Jarvis, C. N. Judice, and W. H. Ninke, "A survey of techniques for the display of continuous-tone pictures on bilevel displays," *Comput. Graph. Image Proc.* **5**, 13-40 (1976).
14. J. O. Limb, "Distortion criteria of the human viewer," *IEEE Trans. Syst. Man Cybern.* **SMC-9**, 778-793 (1979).
15. H. L. Alder and E. B. Roessler, *Introduction to Probability and Statistics*, 6th ed., W. H. Freeman and Company, San Francisco, CA (1977).



Meng Yao received the BS degree in biomedical engineering from Southeast University, Nanjing, China, in 1989 and the MS in electrical engineering from the University of Rochester in 1991. Currently, he is working toward his PhD in the field of digital halftoning at the University of Rochester.



Kevin J. Parker received the BS degree in engineering science, summa cum laude, from the State University of New York at Buffalo in 1976. His graduate work in electrical engineering was done at the Massachusetts Institute of Technology, with MS and PhD degrees received in 1978 and 1981. From 1981 to 1985 he was an assistant professor of electrical engineering at the University of Rochester; currently he holds the title of professor of electrical engineering and radiology. Dr. Parker has received awards from the National Institute of General Medical Sciences (1979), the Lilly Teaching Endowment (1982), the IBM Supercomputing Competition (1989), and the World Federation of Ultrasound in Medicine and Biology (1991). He is a member of the IEEE Sonics and Ultrasonics Symposium Technical Committee and serves as reviewer and consultant for a number of journals and institutions. He is also a member of the IEEE, the Acoustical Society of America, and the American Institute of Ultrasound in Medicine. Dr. Parker's research interests are in medical imaging, linear and nonlinear acoustics, and digital halftoning.